Electronic Supplementary Material (ESI) for Physical Chemistry Chemical Physics.

Supplementary information for

Electrochemistry of Ferrocene Derivatives at Highly Oriented Pyrolytic Graphite (HOPG): Quantification and Impact of Surface Adsorption

Anatolii S. Cuharuc,[†] *Guohui Zhang*[†] *and Patrick R. Unwin**

Department of Chemistry, University of Warwick, Coventry, CV4 7AL, United Kingdom

[†]The authors contributed equally.

* To whom correspondence should be addressed. E-mail: p.r.unwin@warwick.ac.uk

Contents

Section S1. Determination of droplet area

We determined the droplet area for each experiment from voltammetric data as described below. According to the basic assumption of the treatment suggested herein, the total current, i_{tot}, is the sum of diffusional, i_{diff}, and adsorptional, i_{ads}, components:

$$i_{tot} = i_{diff} + i_{ads} \quad \text{(S1)}$$

or considering that peak current $i_{p,diff}$ is proportional to $v^{1/2}$ (Randles-Sevcik equation[1]) and $i_{p,ads}$ to v, one can write

$$i_{p,tot} = aAv^{1/2} + bv$$

or

$$\frac{i_{p,tot}}{av^{1/2}} = A + b'v^{1/2} \quad \text{(S2)}$$

where $a = 2.69 \times 10^5 \, n^{3/2} \, D^{1/2} \, c_0$, A is droplet area, $b' = b/a$ and b is a coefficient of proportionality as defined in eq 10 in the main text. Thus according to eq S2, $i_{p,tot}/av^{1/2}$ *vs* $v^{1/2}$ should yield a straight line with the intercept giving droplet area. In Figure S1, we exemplify several "droplet area plots" for $FcTMA^+$ and FcCOOH. Some are linear throughout the range of scan rates, while others deviate a little from expected behaviour at high scan rates so that only the part corresponding to slow scan rates was fitted to a straight line. The validity of this approach was checked in some cases by measuring the approximate area optically.

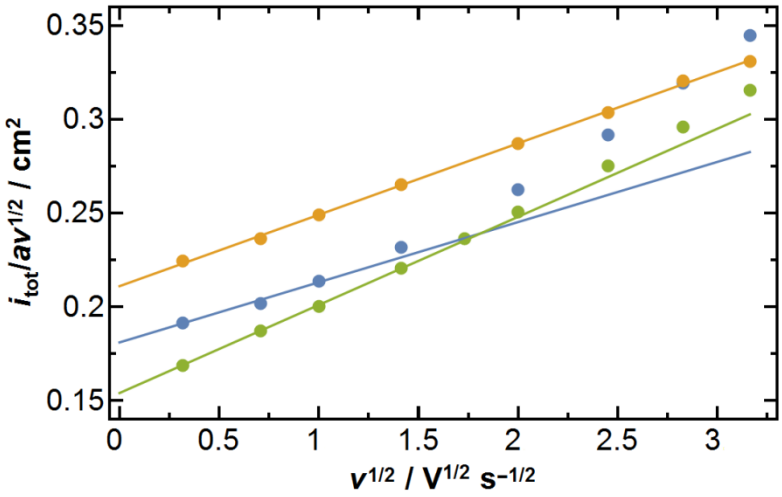

Figure S1. Representative linearization plot for determination of droplet area according to eq S2 with fitting lines for $FcTMA^+$ (blue and orange) and FcCOOH (green).

Section S2. Diffusion coefficients

The diffusion coefficients of $FcTMA^+$ and $FcTMA^{2+}$ ($FcTMA^+$ initially present with c_0 = 1.5 mM) in 1 M KCl were determined via double potential-step chronoamperometry at a Pt UME (radius, a = 14.2 μm, RG > 10, as measured with an optical microscope). A typical chronoamperometric transient of the first potential step (full-driving oxidation of $FcTMA^+$ to $FcTMA^{2+}$) is shown in Figure S2a along with background transient recorded in (pure) 1 M KCl. The experimental data were fitted to eq S3 that describes the diffusion-limited current at a UME[2] (Figure S2b). The value obtained from this fit is $D = 6.7 \times 10^{-6}$ cm^2 s^{-1}. The diffusion coefficient of the oxidized form was found by modelling the diffusion-limited response of the system after the potential was stepped back to fully drive the reduction of $FcTMA^{2+}$ generated during the first step, to $FcTMA^+$ as described elsewhere.[3] In our laboratory, as a part of another project in progress, the diffusion coefficient for this species was also determined via the combination of scanning electrochemical microscopy in feedback mode with substrate-generation/tip-collection mode (results to be published), following

methodology described elsewhere.[4,5] The average value from the two aforementioned techniques was 6.2 × 10^{-6} cm^2 s^{-1}, which is used in the present work. The value for the diffusion coefficient of the Red form is broadly in agreement with values previously published in the literature.[6–8]

The diffusion coefficient for $FcCH_2OH$ (c_0 = 0.5, 0.75 and 1 mM in 1 M KCl) was determined from the limiting current at the same electrode and amounted to D = 6.5 × 10^{-6} cm^2 s^{-1}. The value for FcCOOH (D = 6.4 × 10^{-6} cm^2 s^{-1}) was taken from the literature[9].

$$i(t) = 4nFaDc_0\left(\pi/4 + \frac{\pi^{1/2}}{2}\frac{a}{2D^{1/2}}\frac{1}{t^{1/2}} + (1-\pi/4)\exp\left[-\frac{\pi^{1/2}/2 - 4\pi^{-3/2}}{1-\pi/4}\frac{a}{2D^{1/2}}\frac{1}{t^{1/2}}\right]\right) \qquad \text{(S3)}$$

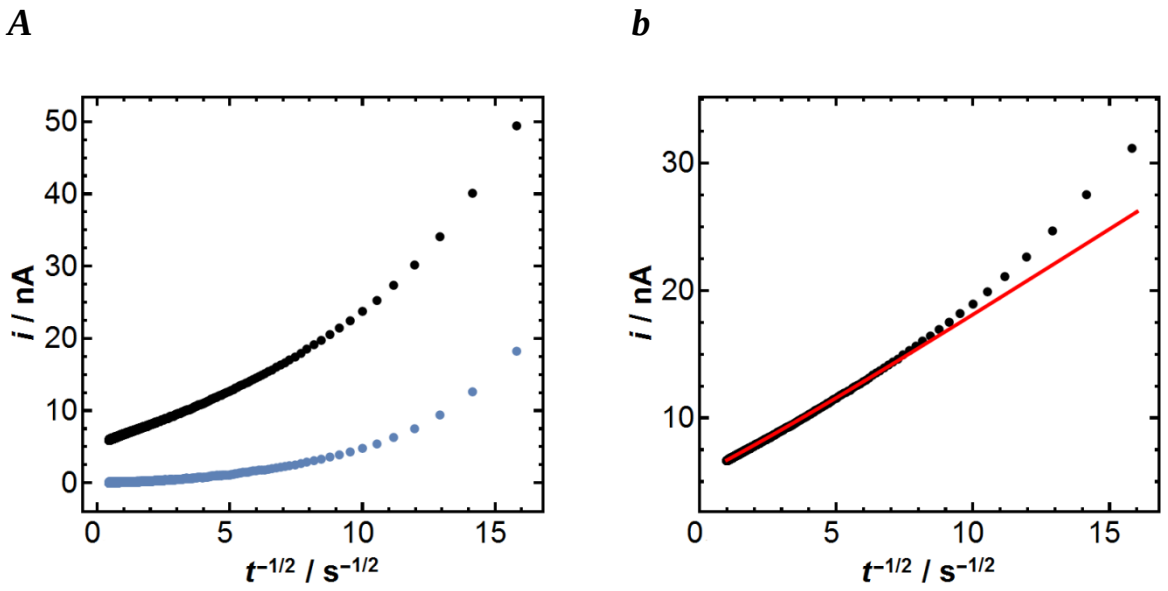

Figure S2. a) Chronoamperometric transients in solution containing 1.5 mM $FcTMA^+$ in 1 M KCl (black) and in pure KCl (blue). b) Background-subtracted transient with the fit according to eq S3.

Section S3. When do equations 11-13 hold true?

Equations 11 – 13 of the main text are the basis of the derivation of the equation for the current from adsorbed Red in the case of the Langmuirian isotherm (eq 19); equally they are foundational for the analysis with the Frumkin isotherm. It thus seemed important to provide a more detailed explanation of their applicability. Below, we focus on the case of the Langmuir isotherm to exemplify the principle we seek to convey.

First, consider the case when the error in the recovery of θ_{in} is very small. As mentioned in the main text, this necessitates low bulk concentration of reactant and low coverages: for c_0 = 0.53 mM, and with corresponding θ_{in} = 0.089, the error in recovery of this value is ~2%. This means that eqs 11 – 13 should hold with high precision. Since we postulated that near-electrode concentrations do not differ to any significant extent between the case of a purely diffusional system and the one with weak reactant adsorption, it is sensible to compare this quantity for these two situations. Near interface concentrations of both Red and Ox were obtained through COMSOL simulations of the voltammetric responses for these cases. Figure S3a plots c_{Red} and c_{Ox} at x = 0 (origin of diffusional layer; near electrode surface) for the cases in question for a scan rate of 6 V s^{-1}. The concentration of Red is only slightly enhanced with adsorption, confirming the validity of the assumption made in the main text. Note, however, that the concentration of Ox in this location is much larger with the adsorption of Red, as a consequence of the conversion of Red_{sol} and Red_{ads} to Ox which diffuses from the electrode. This is especially true for E > ~ 0.4 V. The exact difference between the concentration-potential profiles for the pure diffusional case and the case with adsorption is given in Figure S3b. Note that the difference for Red reaches ~ 0.045 mM, which, in relative terms, is ~16 %. Whether this is significant or not becomes clear when the case of large error in θ_{in} is considered.

For c_0 = 21.7 mM, with corresponding θ_{in} = 0.80, the error in the recovery θ_{in} is more considerable, constituting ~16% (see also error plot in the main text, Figure 2). In a similar fashion, we plotted the Red and Ox profiles and their difference in Figure S3c and d. Surprisingly, both c_{Red} and c_{Ox} for the pure diffusional case and the one with adsorption are in closer agreement, compared to the previous case. This may initially seem counterintuitive as the error in θ_{in} is eight times larger than for the case outlined above. The relative difference in the Red concentration-potential profile reaches only ~2%. In fact, such behaviour is understandable since with higher c_0 the diffusional contribution to the electrochemical current dominates much more over the adsorptional one. Clearly eq 12 and 13 are more precise in this case (relative error decreases). However, the validity (or accuracy) of eq 11, when the true c_{Red} is approximated by the diffusion-controlled quantity, decreases for higher c_0 (and higher θ_{in}). What is important is not the relative accuracy of interfacial c_{Red} (for it is this quantity that enters eq 11) with respect to bulk, but the absolute one and the accuracy decreases for higher bulk concentration, as can be easily seen by comparing Figure S3b with d. If this statement is not obvious from the form of eq 11, we prove the point by taking a finite difference of eq 11 between the pure diffusional case and the one with adsorption:

$$\Delta\Gamma \approx \frac{d\Gamma}{dc_{Red}}\Delta c_{Red} = \frac{\Gamma_{max}K}{(1+Kc_{Red})^2}\Delta c_{Red} \qquad \text{(eq S4)}$$

where $\Delta\Gamma = \Gamma_{exact} - \Gamma_{approx}$, and $\Delta c_{Red} = (c_{Red})_{exact} - (c_{Red})_{approx}$. By "exact", we mean that the quantity from exact solution of the boundary value problem (eq 1 - 6), which includes adsorption. "Approx" means that the numerical solution is taken from the pure diffusion-controlled problem. The first multiplier from the product in the right-hand side, $\Gamma_{max}K/(1+Kc_{Red})^2$, becomes more accurate with increasing c_0 since $(c_{Red})_{approx} \rightarrow (c_{Red})_{exact}$ but the second one, Δc_{Red}, is the absolute difference between the approximate and exact solutions,

which, as discussed above, increases for larger c_0. This is sufficient to explain larger error in the recovery of θ_{in} with increasing bulk concentration.

All that is outlined in this section above can be summarized very simply: the amount of adsorbed reactant is measured as a difference between the current profiles (peak currents) and this difference is progressively less accurate with increasing $c_{0,}$ as clearly exemplified from the profiles of Red and Ox.

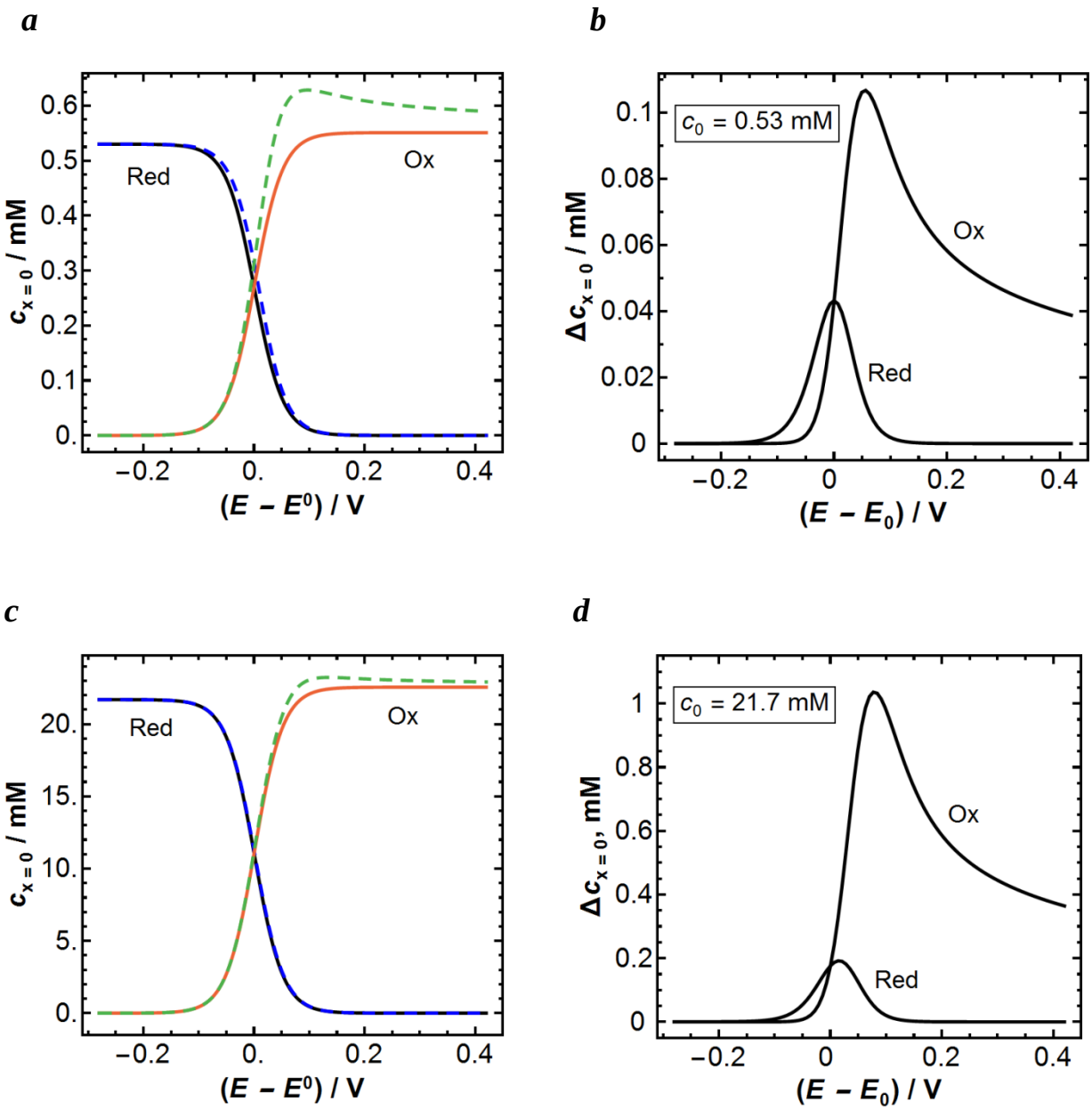

Figure S3. Near-electrode (x = 0) concentration-potential profiles of Red and Ox species are compared for the case of purely diffusional electrode reaction and that complicated by weak adsorption of a reactant (Red). *a*) Red and Ox profiles for c_0 = 0.53 mM, corresponding θ_{in} = 0.09: Red for pure diffusional case (solid black line), Red for adsorption case (dashed blue line), Ox for pure diffusional case (solid red line), Ox for the adsorption case (green dashed line). *b*) Difference in concentration-potential profiles between pure diffusional and adsorption cases for Ox and Red species (same bulk concentration as in *a*. *c*) Red and Ox profiles for c_0 = 21.7 mM, with corresponding θ_{in} = 0.80: Red for pure diffusional case (solid black line), Red for adsorption case (dashed blue line), Ox for pure diffusional case (solid red line), Ox for adsorption case (green dashed line). *d*) Difference in concentration-potential profiles between pure diffusional and adsorption cases for Ox and Red species (same bulk concentration as in *c*).

Section S4. Testing the semi-integration approach

The semi-integration approach for evaluating the adsorption of electroactive species on an electrode, suggested in the literature,[10] is based on several premises: i) concomitant adsorption of both the reduced and oxidized form during the sweep of the potential, ii) Nernstian (fast) electron transfer, iii) bulk concentration of redox species is low, and iv) adsorption is weak. This allowed the use of a simple expression for $d\Gamma/dt$ by implementing the Nernstian process for surface-bound species in the equation for flux, which finally led to a simple formula (in the limit of $t \to \infty$) for the semi-integrated current, I (eq S5; written with relevant adaptations) as a function of time, known experimental parameters, and surface concentration.

$$I = nF(c_{0,\mathrm{Red}}\sqrt{D_{\mathrm{Red}}} + \frac{\Gamma_{\mathrm{Red}}}{\sqrt{\pi t}}) \qquad \text{(S5)}$$

When $t \to \infty$ or, equivalently, $t^{-1/2} \to 0$, Γ_{Red} can be found from the slope of an I vs $t^{-1/2}$ plot. For a CV without adsorption, the slope should be zero and the intercept is $nFc_{0,\mathrm{Red}}\sqrt{D_{\mathrm{Red}}}$, which is indeed what one obtains from semi-integration of purely diffusional wave.[2]

We computed an LSV complicated by weak adsorption of only reactant (Red in our case), shown in Figure S4a, curve *1*. The model parameters were given the following numerical values: $D_{\mathrm{Red}} = 6.7 \times 10^{-6}$ cm^2 s^{-1}, $D_{\mathrm{Ox}} = 6.2 \times 10^{-6}$ cm^2 s^{-1}, $c_0 = 0.25$ mM, $k_0 = 5$ cm s^{-1}, $\alpha = 0.5$, $E^{0\prime} = 0.38$ V, $v = 1$ V s^{-1}, $n = 1$, $\Gamma_{\max} = 5 \times 10^{-10}$ mol cm^{-2}, $K_0 = 735$. This corresponds to initial coverage $\Gamma_{\mathrm{in}} = 5 \times 10^{-11}$ mol cm^{-2} (10 % of a monolayer) and the effect of adsorption is fairly pronounced as can be appreciated by comparing this wave with the one uncomplicated by adsorption (curve *2*; computed using the same parameters except for those relevant for adsorption). If we perform semi-integration as given by eq S6 (ref[2])

$$I = \frac{1}{\sqrt{\pi}} \int_0^t \frac{j(u)}{\sqrt{t-u}}\, du \qquad \text{(S6)}$$

where j is the current density, and plot I vs $t^{-1/2}$ for both LSVs, then the ensuing curves do show linear behaviour as expected from eq S5, but the surface coverage recovered for the profile of I complicated by adsorption (curve *1* in Figure S4b) is 2.4×10^{-10} mol cm^{-2}, which is ~5 times larger than the actual value used to create the simulated result. The value for D_{Red} calculated from the intercept of purely diffusional I (curve *2* in Figure S4b) is 6.86×10^{-6} cm^2 s^{-1}, which corresponds to an error of only 2.4%, showing that the procedure was performed correctly.

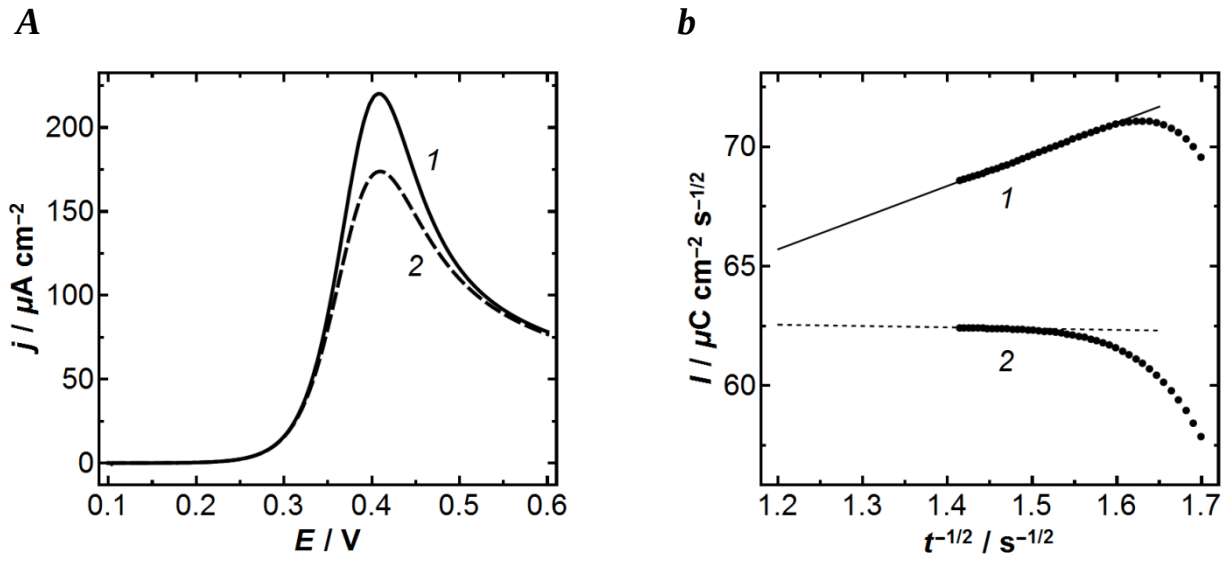

Figure S4. *a*) LSVs in the presence of reactant adsorption (curve *1*) and without such (curve *2*). *b*) Semi-integrated current plotted vs $t^{-1/2}$ for the curves shown in *a*. The straight lines correspond to a limiting behaviour of both semi-integrated curves (*1*: $y = 49.8 + 13.3x$; *2*: $y = 63.2 - 0.537x$).

Section S5. Background currents

As mentioned in the main text, the background currents in the absence of redox and surface active $FcTMA^+$ differed appreciably from those in pure electrolyte solution. This can

be easily seen from the Figure S5 where the regions of the CVs before the beginning of the faradaic process in solutions with and without the redox mediator are compared. Significantly, the slopes of the non-faradaic regions on the CVs with the redox molecule are different from, and steeper than, those in pure KCl. Clearly, the double layer capacitance depends on the potential and presence of the adsorbate and thus extrapolation of the background current from this essentially non-faradaic region to the region where the faradaic current flows is not the most reliable procedure, but perhaps the only option to account for background/capacitative currents.

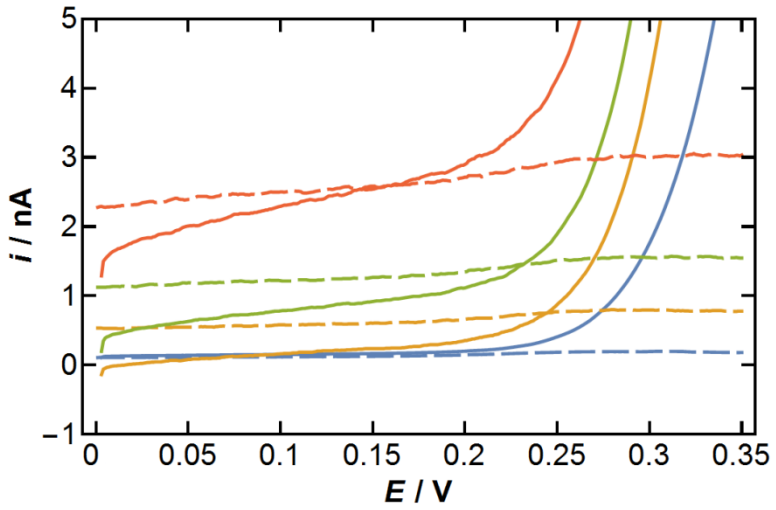

Figure S5. Forward wave of CVs in solutions containing 0.25 mM $FcTMA^+$ (continuous lines) and 1 M KCl only (dashed lines) at scan rates of 0.1 (blue), 0.5 (yellow), 1 (green) and 2 V s^{-1} (red).

References

1 C. M. A. Brett and A. M. Brett, *Electrochemistry: principles, methods, applications*, Oxford University Press, New York, 1993.

2 A. J. Bard and L. R. Faulkner, *Electrochemical Methods: Fundamentals and Applications*, John Wiley&Sons, Inc., New York, 2nd ed., 2001.

3 J. V. Macpherson and P. R. Unwin, *Anal. Chem.*, 1997, **69**, 2063–2069.

4 R. D. Martin and P. R. Unwin, *J. Electroanal. Chem.*, 1997, **439**, 123–136.

5 R. D. Martin and P. R. Unwin, *Anal. Chem.*, 1998, **70**, 276–284.

6 P. Bertoncello, J. P. Edgeworth, J. V. Macpherson and P. R. Unwin, *J. Am. Chem. Soc.*, 2007, **129**, 10982–10983.

7 I. Dumitrescu, P. R. Unwin, N. R. Wilson and J. V. Macpherson, *Anal. Chem.*, 2008, **80**, 3598–3605.

8 J. L. Conyers and H. S. White, *Anal. Chem.*, 2000, **72**, 4441–4446.

9 D. T. Pierce, P. R. Unwin and A. J. Bard, *Anal. Chem.*, 1992, **64**, 1795–1804.

10 M. S. Freund and A. Brajter-Toth, *J. Phys. Chem.*, 1992, **96**, 9400–9406.